

文章编号:1000-0550(2019)02-0254-14

DOI: 10.14027/j.issn.1000-0550.2018.139

砾质辫状河型冲积扇岩相类型、成因及分布规律 ——以准噶尔盆地西北缘现代白杨河冲积扇为例

靳军^{1,2}, 刘大卫^{1,3}, 纪友亮¹, 杨召², 高崇龙¹, 王剑², 段小兵¹, 桓芝俊¹, 罗妮娜¹

1. 中国石油大学(北京)地球科学学院, 北京 102249

2. 中国石油新疆油田分公司实验检测研究院, 新疆克拉玛依 834000

3. 中国科学院地质与地球物理研究所, 北京 100029

摘要 冲积扇砂砾岩储层是准噶尔盆地一类重要的油气储层类型, 由于其具岩相类型多、连续性差等特点, 对冲积扇内部岩相成因解释一直是冲积扇相带认知的基础和难点。以准噶尔盆地西北缘现代白杨河冲积扇为例, 在大量的野外露头资料和粒度分析数据的基础上, 结合冲积扇源区母岩类型、水文资料以及冲积扇文献资料, 对现代白杨河冲积扇岩相的类型、成因及分布规律进行探讨。按沉积机制, 白杨河冲积扇属于辫状河型冲积扇, 具有规模大(扇体总面积约 327.6 km²), 坡度平缓(约 1‰~7‰), 沉积粒度粗等特征。在白杨河冲积扇内共可识别出 16 种岩相类型, 并根据岩相形成的流体动力差异划分为 5 类成因, 即重力流成因、高流态牵引流成因、低流态牵引流成因、静水沉积成因以及风成沉积成因。重力流以洪流沉积为主; 高流态牵引流主要包括片流沉积和湍流沉积; 低流态牵引流以砂(砾)质河道沉积为主; 静水沉积以蓄水细粒沉积为主; 风成沉积以风携细粒沉积为主。根据各岩相沉积构造、粒度特征及展布规模, 可将岩相划分为四类: I 类岩相沉积构造特征明显并具有较大展布规模; II 类岩相沉积构造特征明显但展布规模局限; III 类岩相为不具层理构造但具有较大展布规模的岩相; IV 类岩相不具层理构造并且展布规模局限。其中 I 类和 II 类岩相多为牵引流成因, 多发育于洪水期扇体扇中、扇缘区域以及间洪期扇体的扇中区域, 并可在地下继承性发育为较好的储集相带。

关键词 辫状河型冲积扇; 岩相类型; 粒度特征; 岩相分布; 支撑砾岩

第一作者简介 靳军, 男, 1970 年出生, 教授级高工, 博士, 石油地质学, E-mail: jinjun @ petrochina.com.cn

通信作者 纪友亮, 男, 教授, E-mail: jiyouliang @ cup.edu.cn

中图分类号 P512.2 **文献标志码** A

0 引言

冲积扇砂砾岩储层是一类重要的油气储层类型, 尤其是准噶尔盆地玛湖凹陷砾岩油田的发现, 越加突出了冲积扇砾岩储层的重要性。近年来, 国内外冲积扇的研究越加系统和细致, 研究手段、研究方法以及研究思路更加多样, 尤其是近些年来对地质灾害、地外星体^[1]、实验模拟^[2-3]、冲积扇内储层展布^[4-6]以及构型单元划分的研究^[7-17], 极大的推动了冲积扇的研究进程。冲积扇的发育受控于沉积自旋回(水动力条件)和沉积异旋回(构造^[18-19]、气候^[20-21]、基准面变化^[22]等)共同作用, 因此在全球不同沉积区, 不同冲积扇(即使同一盆地内发育的冲积扇)内岩相类型和发育规律也存在差异。在国内外, 通常根据沉积基质的差异, 将冲积扇的类型划分为以重力流成因岩相为主的泥石型冲积扇^[23-26], 以牵引流成因岩相为主河

流型冲积扇^[27-33], 以及无流水参与(岩体崩落或雪崩)成因岩相类型为主的岩崩型冲积扇^[34-35]。由此看来, 对各类冲积扇内部岩相类型的划分及成因解释就显的尤为重要, 因为冲积扇内岩相可直观反映沉积水动力条件, 还原扇内沉积环境, 甚至可以预测优质相带展布规律。在油气勘探上, 对冲积扇砂砾岩储层取芯井段岩相的正确识别有助于厘定钻遇扇体类型, 从而判定钻遇沉积相带类型并进一步建立储层展布模型。

本文以准噶尔盆地西北缘现代白杨河冲积扇为例, 在大量的野外露头资料、文献资料和粒度分析数据的基础上, 对现代白杨河冲积扇内出露的岩相类型及成因进行归纳阐释, 并总结各岩相粒度特征和展布规律, 旨在阐释辫状河型冲积扇各类岩相沉积条件, 为井下砂砾岩储层的勘探提供丰富的野外资料和理论支撑。

收稿日期: 2017-10-25; 收修改稿日期: 2018-06-05

基金项目: 国家自然科学基金项目(41672098, 41602133) [Foundation: National Natural Science Foundation of China, No. 41672098, 41602133]

1 区域地质概况

白杨河冲积扇位于准噶尔盆地西北缘的和什托洛盖盆地内的白杨河凹陷中(图1),为第四纪时期沉积^[36-37]。研究扇体扇体规模巨大,横向展布长度约36~38 km,纵向展布长度约19~27 km,扇面坡度平缓(1‰~7‰),露头出露条件较好。白杨河冲积扇北邻的乌克兰嘎尔山脉和谢米斯台山脉为主要供源山体,山体内部供源流域面积巨大(约15 508 km²),南邻扎伊尔山脉^[38]。研究区现今扇面可见多条断层活动,扇上供源河流下切形成现今的山区河流—白杨河谷。本次研究扇上共勘探点位100余个,挖掘野外探槽8条,对扇体各区域(扇根、扇中、扇缘区域)进行细致观测。

2 岩相类型及成因解释

根据沉积物类型、沉积构造及水动力条件,在白杨河冲积扇内共识别出16种岩相类型,岩相命名符号的依据 Miall 的岩相分类命名并有所修改。岩相类型依据沉积物形成时的流体动力差异划归为5类成因,即重力流成因、高流态牵引流成因、低流态牵引流

成因、静水沉积成因以及风成沉积成因(图2~5),各类岩相形态及粒度特征详见图3-1和图3-2。

2.1 重力流成因岩相

杂基支撑砾岩(Gmm)岩相为杂基支撑结构,具有反粒序特征,成分主要以中砾—粗砾为主,磨圆中等,砾石多为次圆状—次棱角状,沉积物内部可见“漂砾”现象,最大砾石直径可达40~50 cm。沉积物分选极差,杂基含量极多,且成分多以粗砂—细砾级为主(图2a,b)。此类岩相为重力流沉积的产物,为泥石流沉积成因^[25,39-41],即泥石流沉积之后少量砾石与细粒砂泥混合快速沉积^[42],或者为阵发性洪水事件或者暴雨导致的沉积物高度聚集并快速沉积的产物。杂基支撑砾岩岩相形态呈厚层席状展布,内部由多期反旋回岩层组成,单个反旋回厚度约2~5 m,总厚度可达一百多米,横向延伸距离可达数公里,岩相概率累积线呈平滑上拱形,低斜率,频率分布直方图呈锯齿状,粒径分布宽区间(-6~6 φ)(图3-1)。扇内杂基支撑砾岩岩相主要分布于扇根靠近出山口处的补给水道内。

块状砾岩(Gcm)岩相为颗粒支撑结构,砾石成分以中砾—粗砾为主,岩相整体呈块状构造,无粒序变

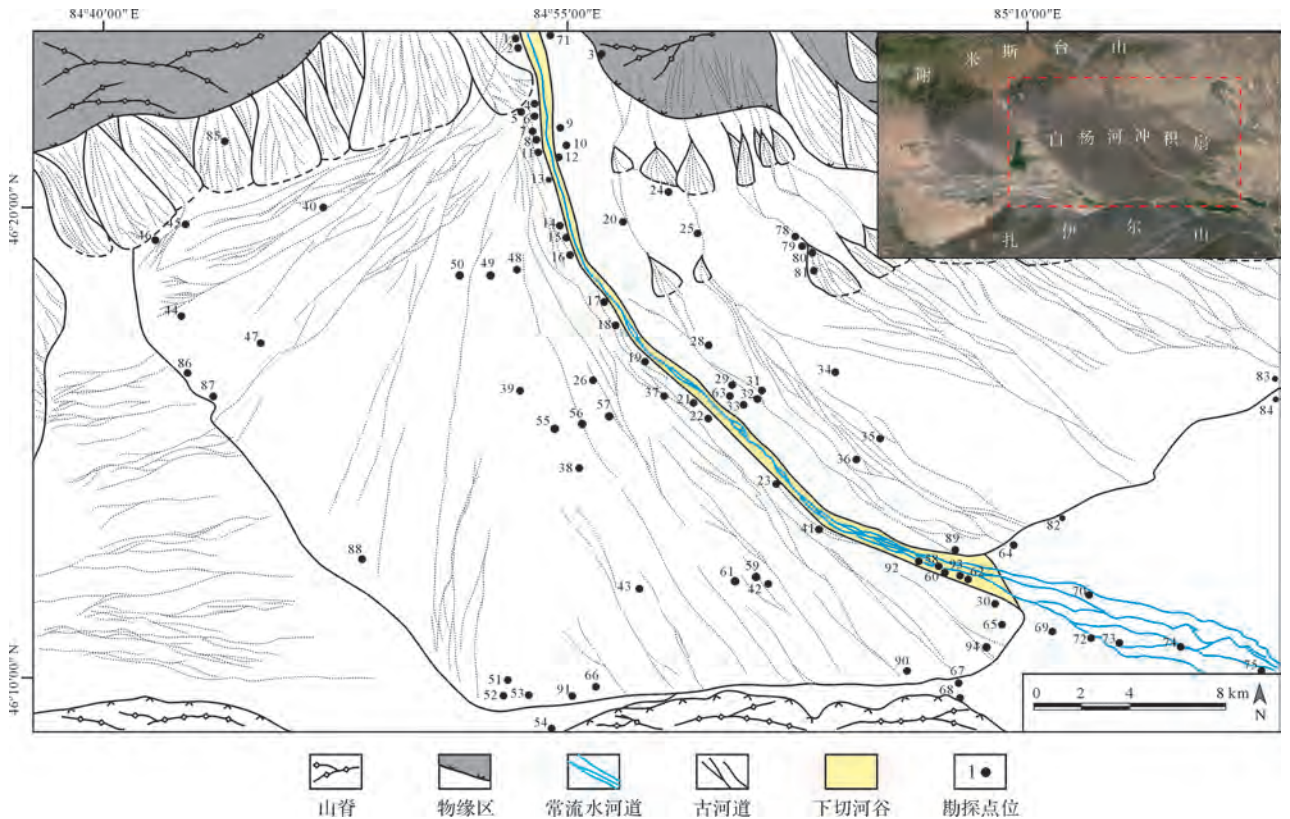


图1 白杨河冲积扇区域地质概况图

Fig.1 Regional geology of Poplar River alluvial fan

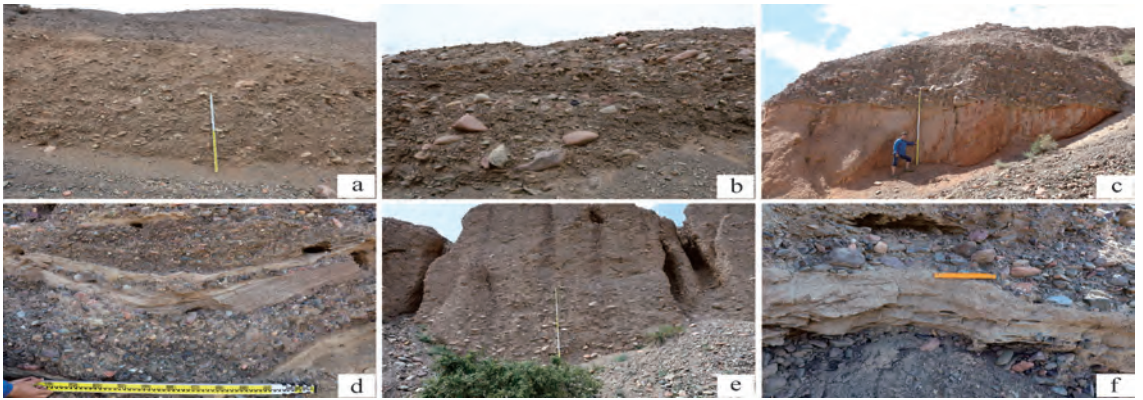


图2 重力流成因岩相野外照片

a.杂基支撑砾岩岩相(Gmm),砾石以中砾—粗砾为主,杂基含量多并以粗砂—细砾为主,重力流沉积成因,厚层层状展布;b.杂基支撑砾岩岩相(Gmm),反粒序,可见大砾石的“飘砾”现象;c.块状砾岩岩相(Gcm),厚层层状,砾石以中砾级为主,杂基以粗砂—细砾为主,洪流沉积物快速卸载成因;d.块状砾岩岩相(Gcm),透镜状,河道底部滞留沉积成因;e.递变层理砾岩岩相(Gcg),厚层层状展布,砾石以中砾—粗砾为主,杂基含量多并以粗砂—细砾为主,为洪水携带沉积物快速堆积而成;f.块状砂岩岩相(Sm),透镜状,中—粗砂为主,短期高密度水流事件成因

Fig.2 Field photographs of debris-flow lithofacies

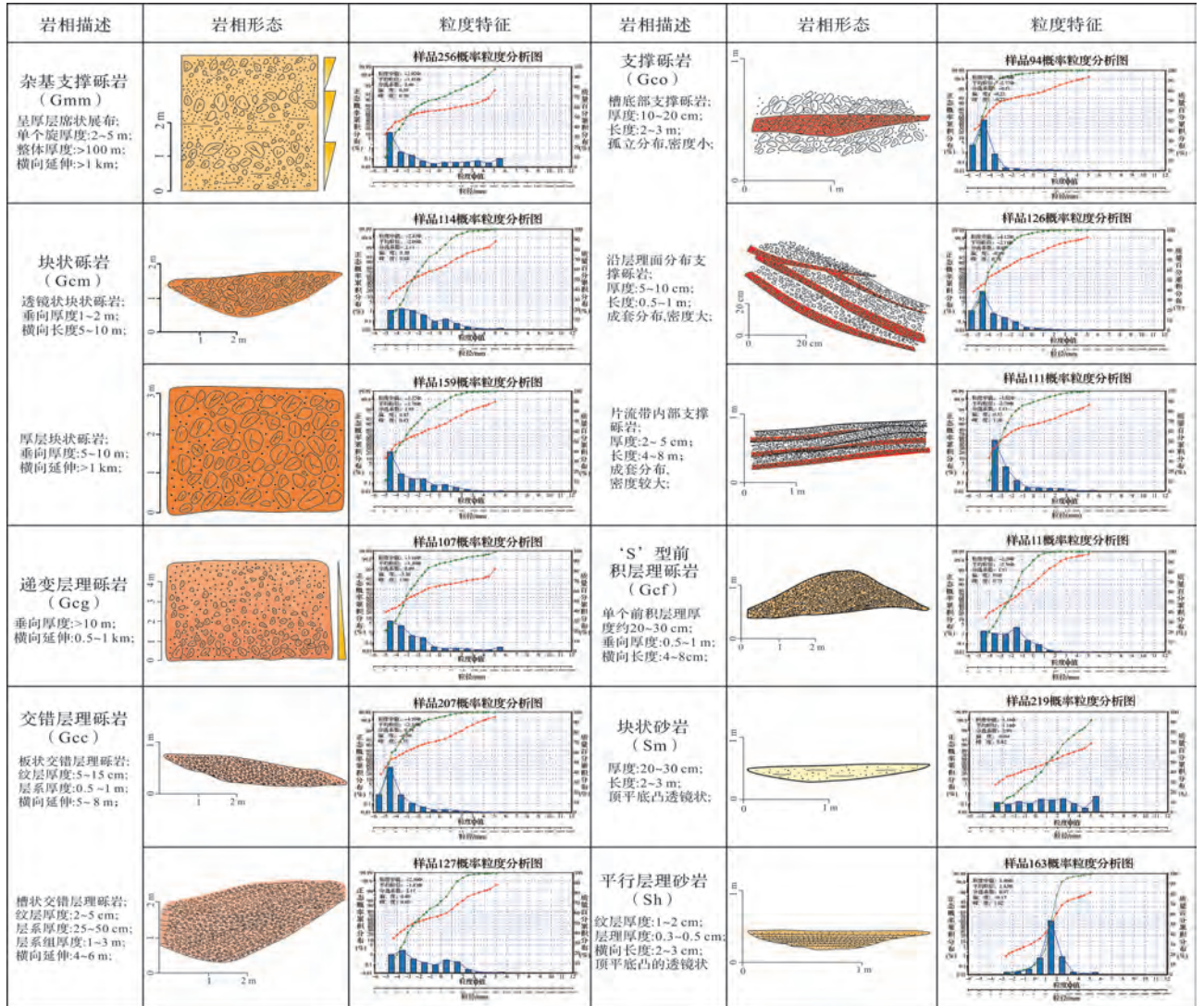


图 3-1 各岩相形态及粒度特征

Fig.3-1 Characteristic of lithofacies form and granularity curve

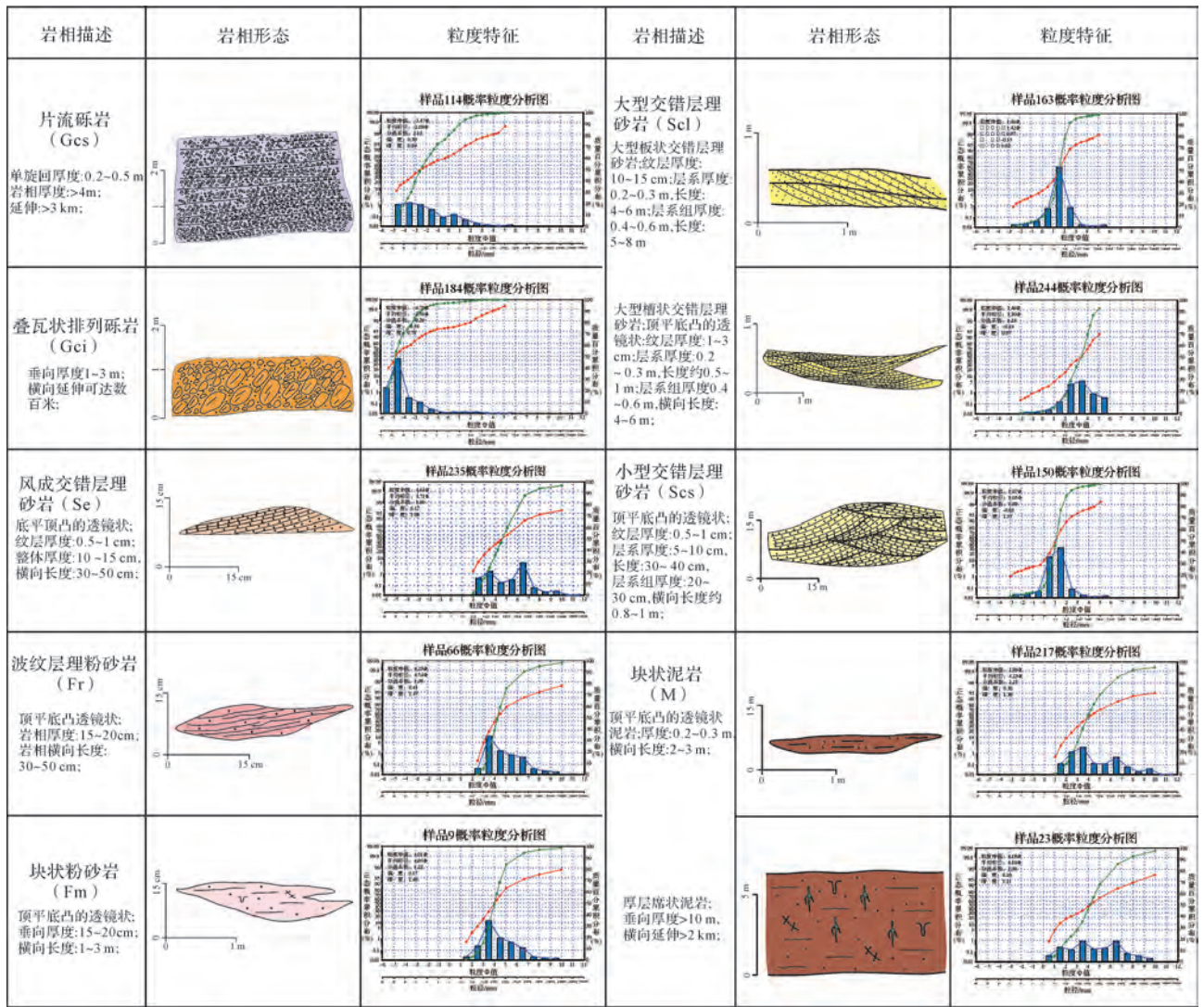


图 3-2 各岩相形态及粒度特征

Fig.3-2 Characteristic of lithofacies form and granularity curve

化,砾石磨圆中等,多为次圆状—次棱角状,最大砾石直径可达 20~30 cm。沉积物分选极差甚至无分选(图 2c, d),砾间杂基多为中砂级—细砾级。此类岩相形成于高流态的水流环境中,为河道内负载沉积产物,或者为水流衰减时期河道底部的滞留沉积产物^[39,41,43-45],块状砾岩岩相同样也可以形成于侵蚀河道底部,即湍流形成的底型沉积。块状砾岩岩相展布形态呈厚层席状或者透镜状,其中呈厚层席状展布岩相垂向厚度可达 5~10 m,横向延伸可达数公里,底部可见明显的冲刷侵蚀面;透镜状块状砾岩岩相分布于河道底部,垂向厚度约 1~2 m,横向长度可达 5~10 m,为河道底部滞留沉积并常见凹形侵蚀面。岩相概率累积曲线呈“简单悬浮一段式”或低斜率两段式,频率分布直方图呈锯齿状,粒度分布宽区间(图

3-1)。扇内块状砾岩岩相主要分布于扇根补给水道内和扇中辫状水道内。

递变层理砾岩(Gcg)岩相为颗粒支撑结构,发育递变层理,呈正粒序,内部偶见薄层条带状砂岩,沉积物内砾石主要为中砾—粗砾级,磨圆中等,多为次圆状—次棱角状,最大砾径达 20~35 cm。沉积物分选极差,砾间杂基含量较多,多为中砂—细砾级(图 2e)。递变层理砾岩岩相形态呈厚层席状展布,垂向厚度可达十几米,横向延伸可达数百米(图 3-1),为洪流所携沉积物快速沉积的产物^[39,45]。扇内递变层理砾岩岩相主要发育于扇根补给水道前缘。

块状砂岩(Sm)岩相为颗粒支撑结构,沉积物成分以中—粗砂为主,含少量细砾,岩相整体呈黄色或淡黄色,内部无层理构造,呈块状构造,沉积物分选较

差(图2f)。块状砂岩岩相(Sm)可反映水流强度衰减期辫状水道内的沉积环境,多代表辫状水道内短期、高密度的水流事件沉积,形成时的水流流态相对较低,为坝顶沉积的标志^[45-46],这类岩相同样可形成于生物扰动作用^[42]。块状砂岩岩相常与块状砾岩岩相、交错层理砾岩岩相相伴生,常可代表一期沉积事件的顶部沉积物,岩相形态多呈顶平底凸的透镜状,规模较小,岩相垂向厚度约20~30 cm,横向延伸可达2~3 m,内部偶见生物钻孔现象。岩样概率累积曲线呈一段式,具较高斜率,频率曲线有2~3个主峰,主峰之间有多个次峰(图3-1)。扇内块状砂岩岩相发育于扇中辫状水道微相内。

2.2 高流态牵引流成因岩相

交错层理砾岩(Gcc)岩相为颗粒支撑结构,发育低角度交错层理(层理倾角 $<5^\circ$),岩相整体呈正粒序,层理底部可见粗砾滞留、柔流变形结构,并可见明显的冲刷侵蚀面。砾石以细砾—中砾级为主,磨圆较好,呈次棱角状—次圆状。砾间杂基含量分布不均,但整体含量较少,杂基多为中砂—粗砂(图4a, b)。交错层理砾岩岩相主要发育于辫状水道沉积环境中,为河床底型迁移(水流流速2~3 m/s)形成的坝体沉积^[32, 44, 47],或是浅河道内坝体的侧向加积物形成的砾质沉积物^[39]。交错层理砾岩岩相根据内部沉积构造差异可进一步划分为槽状交错层理砾岩岩相、板状交错层理砾岩岩相,其中槽状交错层理砾岩岩相较为常见,岩相内部纹层厚度约2~5 cm,层系厚度约25~50 cm,层系组厚度可达1~3 m,横向延伸可达4~6 m;板状交错层理砾岩岩相常孤立出露,但规模较大,内部纹层厚度约5~15 cm,层系厚度约0.5~1 m,横向延伸可达5~8 m。岩样概率累积曲线呈“一滚两跳—悬浮”特点,频率分布直方图为宽区间特征,频率曲线具有多个主峰,标准偏差1~2.4,峰度0.56~1.25(图3-1)。扇内交错层理砾岩岩相主要发育于扇体发育间洪期的主槽和辫状沟槽沉积微相内。

片流砾岩(Gcs)岩相为颗粒支撑结构,砾石多为细砾—中砾级,分选较差,磨圆中等,次棱角状—次圆状,岩相整体呈正粒序,单层底部可见局部低角度排列的砾石(倾角约 $2^\circ\sim5^\circ$),砾间杂基多为中—粗粒级砂岩(图4c, d)。这类岩相形成于高流态水动力条件下($V_{水}\approx3\sim6\text{ m/s}$)河道内或非限制河道内,是超临界扩散水流条件下,漫洪沉积的产物^[48]。片流砾岩岩相呈厚层席状展布,内部可见多套正韵律薄层砂砾岩互层叠置,多期叠置厚度大于4 m,横向延伸距

离大于3 km。岩样概率累积曲线呈平滑上拱形,低斜率,频率分布直方图显示粒度分布区间较宽,多峰,标准偏差1.65~2.42,峰度0.16~0.46,沉积物主体为跳跃组分(图3-2)。片流砾岩岩相主要发育于扇根片流带微相以及扇中片流带微相内。

叠瓦状排列砾岩(Gci)岩相为颗粒支撑结构,砾石以中砾—粗砾级为主,分选较差,磨圆中等,次棱角状—次圆状,砾间杂基含量较多,粒级为极粗砂—细砾级。岩相整体呈正粒序,内部砾石具叠瓦状排列现象,向源倾斜,砾石倾角约 $20^\circ\sim30^\circ$ (图4e, f)。这类岩相形成于高流态水流条件下的主河道底部环境^[41]。叠瓦状砾岩岩相形态呈席状展布,常与块状砾岩岩相伴生,底部可见明显的冲刷侵蚀现象,该岩相垂向厚度约1~3 m,横向延伸可达数百米(图3-2)。叠瓦状排列砾岩岩相主要发育于扇根补给水道微相以及扇中辫状水道微相底部。

支撑砾岩(Gco)岩相为颗粒支撑(岩石骨架支撑)结构,砾石主要为细砾—中砾级,少见粗砾级,分选较好,磨圆中等,次棱角状—次圆状,砾间杂基含量极少甚至不含杂基。岩相整体呈正粒序,砾间孔洞发育,并具有一定规模与延伸距离(图4g, h, i)。支撑砾岩的命名并未采用“沉积构造+岩性”命名规则,而是采用“结构样式+岩性”命名原则,一方面是为了不与递变层理砾岩命名相混淆,突出其骨架颗粒间杂基含量极少的特点,国内外也将这类岩相命名为“骨架砾岩”、“洪积砾岩”;另一方面支撑砾岩形成水动力条件为溢散的超临界水流,而非牵引流下砂波底型迁移的结果,故而不能套用“沉积构造+岩性”的命名原则。支撑砾岩岩相主要发育于限制性的辫状水道环境中,为河道内常流水区湍流持续淘洗产物,或者形成于超临界水流条件下,水流对底部沉积物的淘洗再沉积作用的产物^[35, 49],该岩相是一类特殊的岩相单元,根据其形成环境和分布样式的差异,将支撑砾岩岩相划分为沿沟槽底部分布支撑砾岩、沿层理面分布支撑砾岩、片流带内分布的支撑砾岩,其中沿沟槽底部分布支撑砾岩孤立分布,厚度约10~20 cm,长度约2~3 m;沿层理面分布支撑常成套分布,分布密度大,单层厚度约5~10 cm,长度约0.5~1 m;片流带内支撑砾岩主要沿片流层面分布,支撑砾岩成套出露且密度较大,单层厚度约2~5 cm,长度约4~8 m。岩相粒度概率曲线呈“高截点两段式”,粒径 $-6\sim1\phi$ 占总体95%以上,频率分布直方图区间较窄,少峰,反映分选较好(图3-1)。扇内支撑砾岩岩相常发育于扇根和



图4 高流态牵引流成因岩相野外照片

a.槽状交错层理砾岩岩相(Gcc),砾石以细砾—中砾为主,砾间杂基以中砂—粗砂为主,河道内底型迁移成因;b.板状交错层理砾岩岩相(Gcc),砾石以细砾—中砾为主,砾间杂基以中砂—粗砂为主,河道内底型迁移成因;c.片流砾岩岩相(Gcs),砾石为细砾—中砾级,杂基为中砂—粗砂,非限制漫洪成因,厚层层状展布;d.单期片流砾岩岩相(Gcs),砾石具定向性,可见递变层理、支撑砾岩现象,薄层状延伸;e.叠瓦状排列砾岩岩相(Gei),砾石以中砾—粗砾为主,砾间杂基以中砂—极粗砂为主,为主槽内高流态水流成因,层状展布;f.叠瓦状排列砾岩岩相(Gei),辫状河内高流态水流成因,砾石倾角 $\angle 20^{\circ} \sim 30^{\circ}$;g.支撑砾岩(Gco),沿沟槽底部分布,砾石以细砾—中砾为主,杂基以中砂为主,为水流淘洗成因,顶平底凸的透镜状(厚0.2 m \times 长2 m);h.支撑砾岩(Gco),片流带内分布,砾石以细砾—中砾为主,杂基以中砂为主,与片流沉积物伴生,超临界水流淘洗成因,条带状(厚0.05 m \times 长5 m);i.支撑砾岩(Gco),沿层理面分布,砾石以细砾—中砾为主,杂基以中砂为主,与沉积层理匹配,超临界水流淘洗成因,呈条带状(厚0.1 m \times 长1 m);j.“S”型前积层理砾岩(Gcf)岩相,砾石主要为细砾—中砾级,砾间杂基含量较高且为中砂—极粗砂,为河道内坝体前积增生成因,底平顶凸的透镜状(厚0.75 m \times 长6 m);k.平行层理砂岩(Sh)岩相,细砂—中砂为主,含少量细砾,河床沙丘底型迁移成因;l.平行层理砂岩岩相(Sh),透镜状(厚0.2 m \times 长1.5 m)夹于砾岩层中,河床底型迁移成因;m.大型交错层理砂岩岩相(Sc1),粗砂—极粗砂,沙丘底型迁移成因,顶平底凸透镜状(厚0.3 m \times 长1.5 m);n.大型交错层理砂岩岩相(Sc1),中砂—极粗砂,具有高角度层理倾角($\angle 10^{\circ} \sim 15^{\circ}$),河床底型迁移成因,顶平底凸透镜状

Fig.4 Field photographs of upper-flow regime lithofacies

扇中的片流带内以及扇中的辫状沟槽微相内。

“S”型前积层理砾岩(Gcf)岩相为颗粒支撑结构,砾石主要为细砾—中砾级,沉积物分选较差,砾间杂基含量较高,杂基多为中砂—极粗砂(图4j),主要形成于河道内坝体迁移侧积^[39]。岩相形态呈底平顶凸的透镜状,整体厚度约0.5~1 m,横向长度约4~

8 m,单个前积层厚度约20~30 cm,沿前积层面可见支撑砾岩岩相分布(图3-1)。扇内“S”型前积层理砾岩岩相主要发育于扇中辫状水道微相内。

平行层理砂岩(Sh)岩相沉积物主要为细砂—中砂级,含少量细砾,分选中等偏好,岩相整体呈土黄色或黄色,整体以及内部层理皆为正粒序,层理呈平

行—低角度的层状,岩石相内部可见生物钻孔和植物根茎,底部可见冲刷侵蚀面,局部存在柔流变形构造(图4k,1)。平行层理砂岩岩相形成于河道内高流态的水动力环境或者向高流态转化的水动力条件下,也可以形成于河道内阵发性洪水沉积或由此产生的溢岸沉积^[27,31,35]。岩相形态呈顶平底凸的透镜状,是河道内较高流态下的沉积产物,岩相内部纹层厚度约1~2 cm,岩相整体规模较小,垂向厚度约0.3~0.5 m,横向长度约2~3 m,内部可见生物钻孔及植物根茎。岩样概率累积曲线为三段式,其中滚动搬运组分所占比例最大(60%~70%),其次是跳跃搬运组分(22%~35%),悬浮搬运组分小于5%,频率分布直方图粒度分布区间窄,单峰,标准偏差0.77~3,峰度0.68~1.67,整体较尖锐,分选较好(图3-1)。扇内平行层理砂岩岩相主要发育于扇中辫状沟槽沉积环境中。

大型交错层理砂岩(Scl)岩相以沉积物以中砂岩—极粗砂岩为主,含少量细砾和中砾,正粒序,分选中等,其中槽状交错层理砂岩和板状交错层理砂岩常见,少见楔状交错层理砂岩,具高角度($\angle 10^\circ \sim \angle 15^\circ$)交错层理倾角以及局部发育的逆向倾角,在大型交错层理砾岩内部可见粗砾滞留、同生变形构造现象(图4m,n)。该岩相一般形成于主河道内平坦河床底部大型波纹和沙坝迁移,形成时的水流流态较高($V_w \approx 0.7 \text{ m/s}$)^[50-52]。大型交错层理砂岩岩相形态为顶平底凸的透镜状,内部可见植物根茎以及生物挖掘痕迹,大型板状交错层理呈板状形态并向两侧逐渐减薄,岩相内部纹层厚度约10~15 cm,层系厚度约0.2~0.3 m,横向延伸约4~6 m,层系组厚度约0.4~0.6 m,横向延伸约5~8 m;大型槽状交错层理整体呈顶平底凸的透镜状,岩相内部纹层厚度约1~3 cm,层系厚度约0.2~0.3 m,长度约0.5~1 m,层系组厚度0.4~0.6 m,横向长度约2~4 m。大型交错层理砂岩岩相概率累计曲线呈四段式,粒度分布区间较宽,以单峰或双峰为特征,标准偏差为1.2~3.5(图3-2)。大型交错层理砂岩岩相常发育于扇中辫状水道微相、扇中辫状沟槽微相以及扇缘径流水道微相内。

2.3 低流态牵引流成因岩相

小型交错层理砂岩(Scs)岩相沉积物以细砂—粗砂为主,含少量细砾,分选中等,整体为正粒序,呈黄色或土黄色。岩相内部多见槽状交错层理,少见板状或楔状交错层理,层理的倾向一致,底部可见明显的冲刷侵蚀面(图5a,b)。该岩相多形成于低流态的水

流条件下,发育于间洪期辫状沟槽沉积环境中^[31-32,42]。岩相形态呈顶平底凸的透镜状,规模较小,主要形成于小规模河道内,岩相内纹层厚度约0.5~1 cm,层系厚度约5~10 cm,长度约30~40 cm,层系组厚度约20~30 cm,横向长度约0.8~1 m。岩样概率累积曲线呈四段式,具两个跳跃总体,频率曲线为单峰,标准偏差1~2,峰度0.5~2(图3-2)。扇内小型交错层理砂岩岩相常发育于扇中辫状沟槽微相内,或者扇缘径流水道中。

波纹层理粉砂岩(Fr)岩相沉积物主要为粉砂,含有少量中细砂岩,分选较好,底部具不明显的冲刷侵蚀面,并具有一定程度的成土作用(图5c)。该岩相常发育于小规模(河道浅)限制性河道内,为流水单元环境中细粒沉积物^[32],也可发育于非限制河道内,为低流态水流中细粒物质运移的沉积产物^[39,42]。岩相形态呈顶平底凸的透镜状,内部可见不明显的波纹层理,岩相规模较小,垂向厚度约15~20 cm,横向长度约30~50 cm(图3-2)。扇内波纹层理粉砂岩岩相常发育于扇缘径流水道微相以及扇缘湿地微相内,代表着河道演化后期的沉积产物。

2.4 静水沉积成因岩相

块状粉砂岩(Fm)岩相沉积物主要为粉砂—细砂级,含有细砾,分选中等,岩相内部无明显的层理构造,呈块状,底部可见冲刷面,颜色为黄色或土黄色。块状粉砂岩岩相常与块状砾岩岩相、交错层理砾岩岩相伴生,常指示单期沉积旋回的顶部沉积物,岩相内部可见植物根茎和生物的挖掘痕迹,具有一定的成土作用(图5d)。该岩相常形成于水流流速急剧减弱时期,是高泥质含量水流中悬浮沉积的产物,该岩相常指示洪水后期或泥石流沉积事件后期阶段^[32,42,50]。块状粉砂岩岩相形态呈顶平底凸的透镜状,规模较小,垂向厚度约15~20 cm,横向长度约1~3 m。岩样概率累积曲线呈两段式,由跳跃组分和悬浮组分构成,频率直方图粒度呈窄区间,单峰或双峰,标准偏差1.22~2.36,峰度1.05~1.47(图3-2)。扇内块状粉砂岩岩相常发育于扇根补给水道微相以及扇中辫状水道微相内,常指示扇上废弃河道沉积。

块状泥岩(M)岩相沉积物以泥岩—粉砂为主,块状构造(图5e, f),为静水条件下细粒沉积物悬浮沉降的沉积产物^[50]。根据岩相形态可分为透镜状泥岩和厚层块状泥岩,其中透镜状泥岩呈顶平底凸形态,主要分布于河道流沟,是河道演化后期的沉积产物,规模较小,垂向厚度约0.2~0.3 m,横向长度可达2~

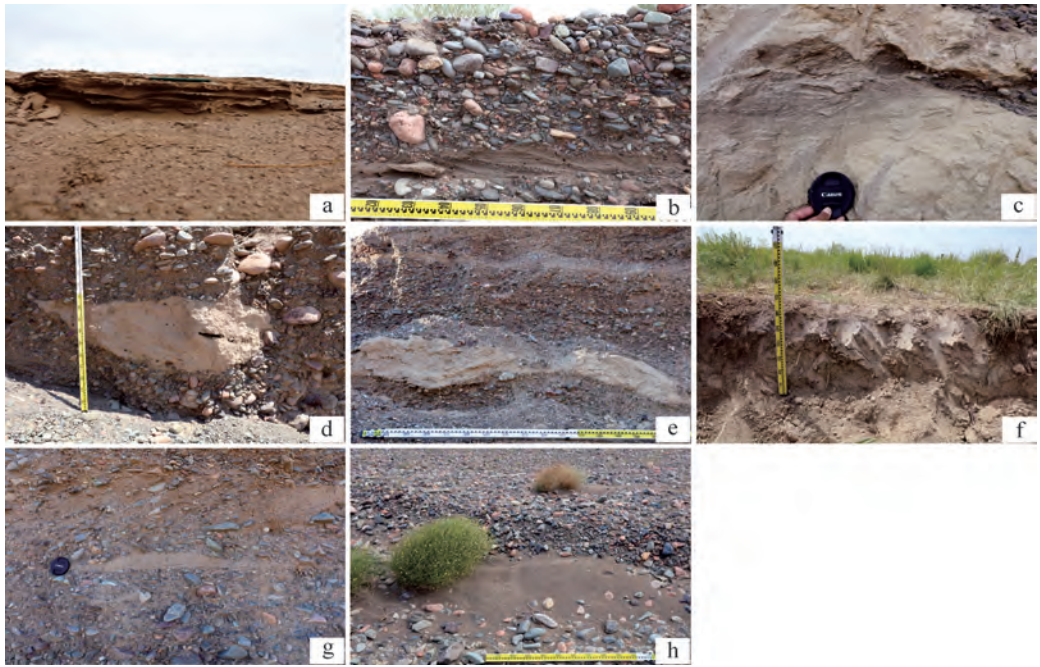


图5 低流态牵引流成因、静水沉积成因及风成成因岩相野外照片

a. 小型交错层理砂岩岩相 (Scs), 细砂—粗砂岩, 发育于地表流沟内; b. 小型交错层理砂岩岩相 (Scs), 细砂—粗砂岩, 发育于砾质坝体内部, 顶平底凸的透镜状 (厚 0.2 m × 长 0.9 m); c. 波状层理粉砂岩岩相 (Fr), 粉砂岩, 低流态水流中细粒推移质的沉积产物; d. 块状粉砂岩岩相 (Fm), 发育于扇根区域砾岩层中, 为局部滞留水体中沉积物悬浮沉降成因, 顶平底凸的透镜状 (厚 0.5 m × 长 2 m); e. 块状粉砂岩岩相 (Fm), 发育于扇中外带砾岩层中; f. 块状泥岩 (M), 静水沉降成因, 扇缘发育, 植被覆盖; g. 风成交错层理砂岩岩相 (Se), 极细砂—中砂, 分选好, 底平顶凸的透镜状 (厚 0.15 m × 长 0.4 m); h. 风成交错层理砂岩岩相 (Se), 发育于扇面植被背风一侧, 透镜状堆积

Fig.5 Field photographs of lower-flow regime, hydrostatic sediment and aeolian lithofacies

3 m; 厚层块状岩相规模较大, 呈厚层席状展布, 岩相垂向厚度可达十几米 (扇缘岩芯资料显示), 横向延伸距离可达数公里, 岩相内部可见大量的植物根茎和生物钻孔现象 (图 3-2)。块状泥岩岩相主要分布于扇上流沟和扇缘湿地内。

2.5 风成成因岩相

风成交错层理砂岩 (Se) 岩相沉积物以极细砂—中砂为主, 分选较好, 显黄色。岩相形态呈底平顶凸的透镜状, 露头出露较少 (图 5g)。风成沉积物往往形成于扇表低洼处^[35], 也可以形成于地表植被的背风侧 (图 5h)。该岩相规模很小, 纹层厚度约 0.5 ~ 1 cm, 整体厚度约 10 ~ 15 cm, 横向长度约 30 ~ 50 cm。岩样概率曲线呈高斜率, 为多个跳跃总体复合的特征, 粒度分布区间较窄, 频率曲线显示单峰, 峰度 1.15 ~ 1.34, 标准偏差为 0.77 ~ 1.22 (图 3-2)。风成交错层理岩相往往发育于扇中和扇缘亚相内, 在扇根亚相内少见, 多分布于扇中辫状沟槽微相、槽间带微相内。

3 岩相分布规律及类型划分

根据冲积扇内岩相分布统计 (图 6、表 1), 片流

砾岩岩相 (Gcs)、交错层理砾岩岩相 (Gcc)、块状砾岩岩相 (Gem) 这 3 类岩相在扇内出露比例大, 出现频率高。在扇根区域, 向扇缘方向主要出露杂基支撑砾岩岩相 (局部占比 45%)、块状砾岩岩相 (45% → 15.5%)、片流砾岩岩相 (4.5% → 41%)、交错层理砾岩岩相 (4% → 33%), 在局部出露递变层理砾岩岩相 (20%)、大型交错层理砂岩岩相 (4%) 以及支撑砾岩岩相 (1%) 等; 扇中区域, 向扇缘方向主要出露块状砾岩岩相 (15% → 27%)、交错层理砾岩岩相 (27% → 49%) 以及片流砾岩岩相 (61% → 6%), 在局部区域出露小型交错层理砂岩岩相 (2.5%)、块状粉砂岩岩相 (1.5%) 及支撑砾岩岩相 (1%) 等; 扇缘区域主要发育块状泥岩岩相 (90%) 和少量次物源砾岩岩相 (10%) (图 7)。

根据各岩相沉积构造、粒度特征及展布规模, 可将岩相大致划分为四类 (表 1): I 类岩相沉积构造特征明显并具有较大展布规模, 如交错层理砾岩 (Gcc) 岩相; II 类岩相沉积构造特征明显但展布规模局限, 如支撑砾岩 (Gco)、交错层理砂岩 (Sc) 岩相; III 类岩相为不具层理构造但具有较大展布规模的岩相, 如块

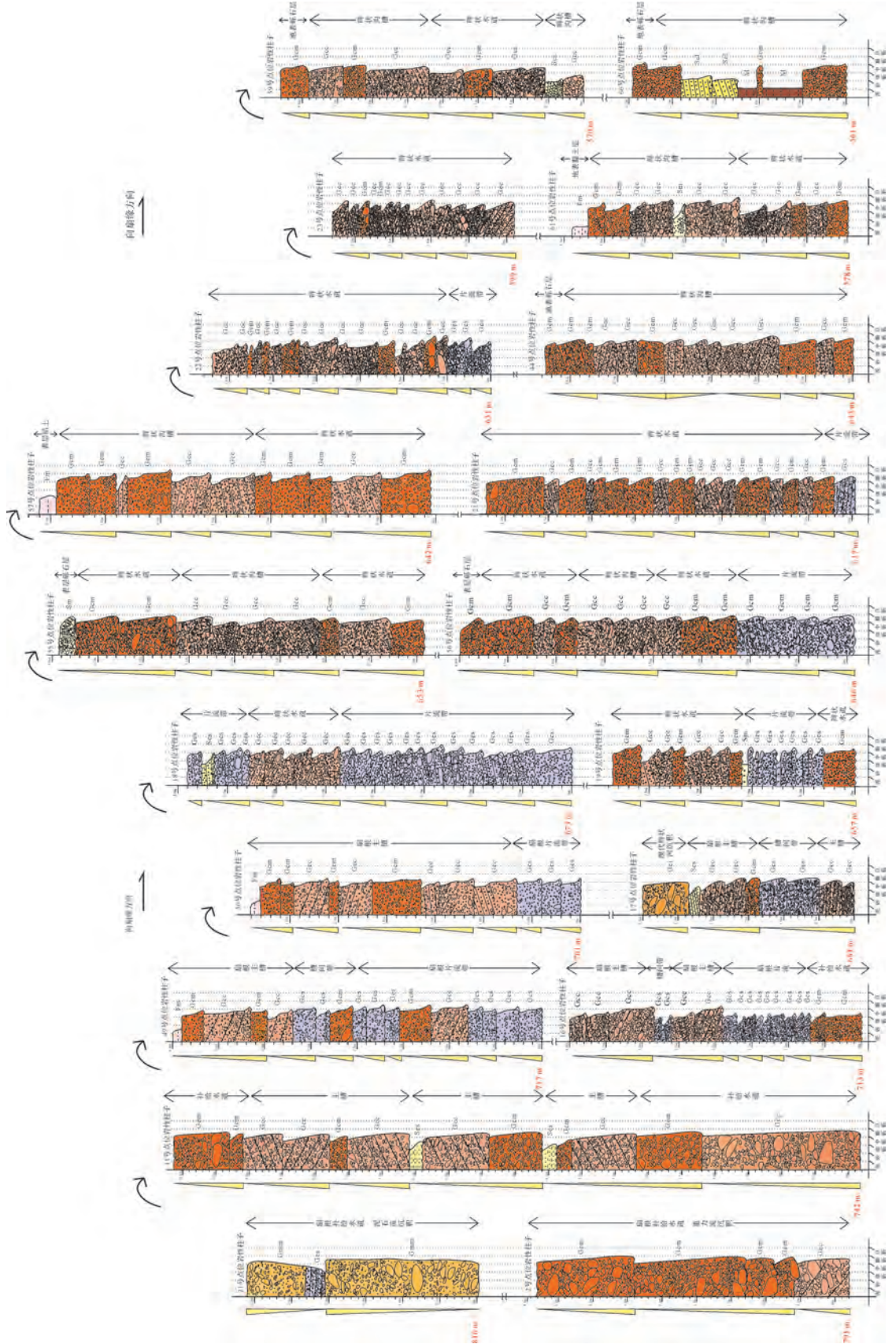


图7 扇根至扇中外带野外实测岩相柱刻画

Fig.7 Lithofacies pillars from proximal to inner external-intermediate part of the alluvial fan

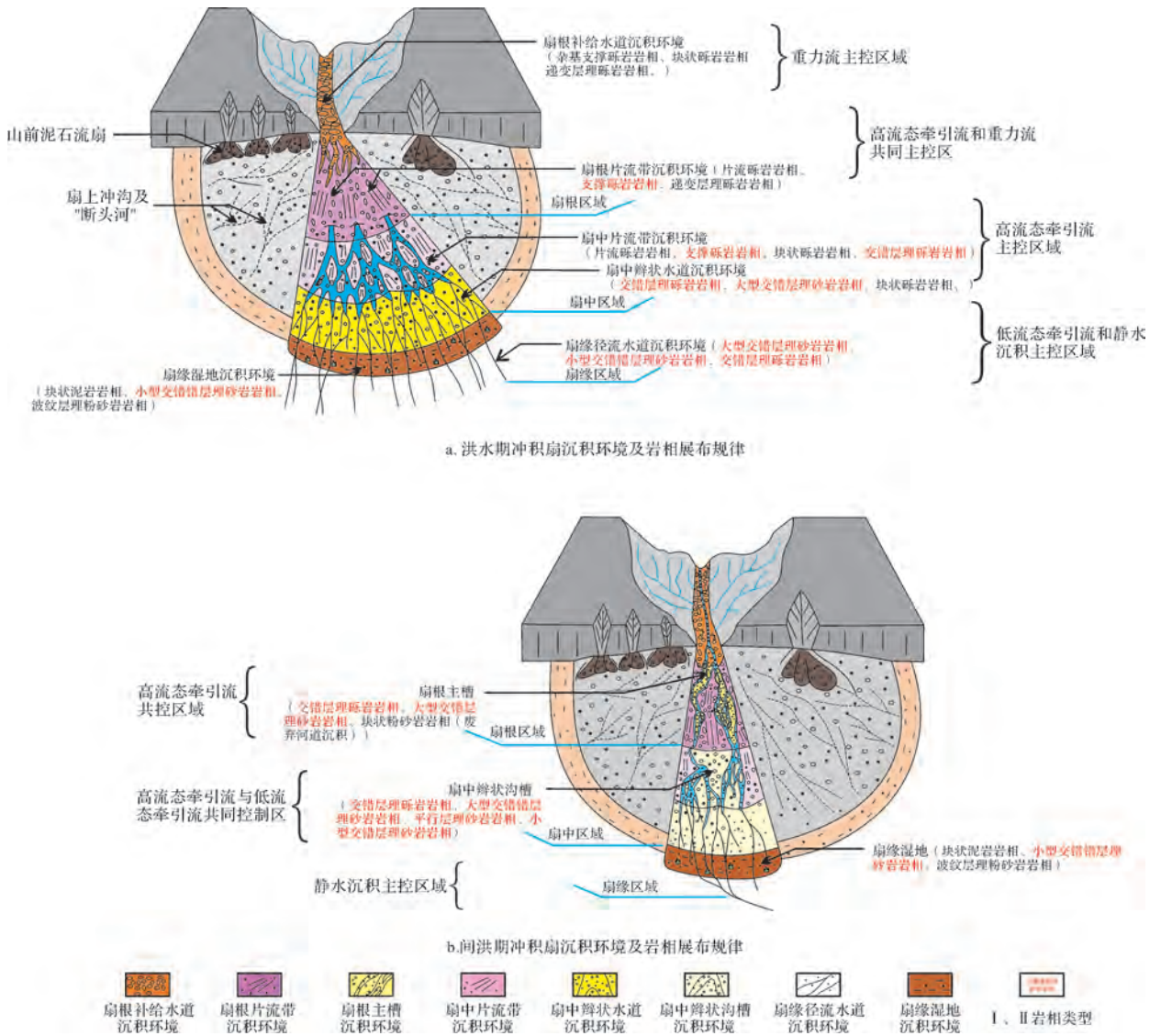


Fig.8 Main sedimentary environments and lithofacies distribution pattern in Poplar River alluvial fan

外带区域) 同样可发育少量优势岩相—支撑砾岩 (Gco) 岩相。

4 结论

(1) 白杨河冲积扇为砾质辫状河型冲积扇, 内部共识别划分出 16 种岩相类型, 根据岩相形成的流体动力差异划归为 5 类成因, 即重力流成因、高流态牵引流成因、低流态牵引流成因、静水沉积成因以及风成沉积成因。其中重力流以洪流沉积为主; 高流态牵引流主要包括片流沉积和湍流沉积; 低流态牵引流以砂 (砾) 质河道沉积为主; 静水沉积以蓄水细粒沉积为主; 风成沉积以风携细粒沉积为主。

(2) 扇根区域主要的岩相类型以杂基支撑砾岩、

块状砾岩、片流砾岩、交错层理砾岩岩相为主; 扇中区域主要的岩相类型以块状砾岩、交错层理砾岩、片流砾岩岩相为主; 扇缘区域主要以块状泥岩岩相为主。

(3) 根据岩相内沉积构造、粒度特征及展布规模, 可将岩相大致划分为四类: I 类岩相沉积构造特征明显并具有较大展布规模, 如交错层理砾岩 (Gcc) 岩相; II 类岩相沉积构造特征明显但展布规模局限, 如支撑砾岩 (Gco)、交错层理砂岩 (Sc) 岩相; III 类岩相不具层理构造但具有较大展布规模, 如块状砾岩 (Gcc)、片流砾岩 (Gcs) 岩相; IV 类岩相不具层理构造并且展布规模局限, 如递变层理砾岩 (Gcg)、杂基支撑砾岩 (Gmm)、块状砂岩 (Sm) 岩相等。其中 I 类和 II 类岩相可继承性发育为地下较好的储集相带, 为优

势勘探岩相。

(4) 优势岩相(I类、II类岩相)主要发育于洪水期的扇中区域和间洪期的扇根以及扇中区域,往往形成于高流态牵引流和低流态牵引流主控的沉积环境内。总的来说,岩相类型及分布规律响应于沉积水动力变化。

参考文献 (References)

- [1] Moore J M, Howard A D. Large alluvial fans on Mars[J]. *Journal of Geophysical Research*, 2005, 110(E4): 1-24.
- [2] 张春生. 冲积体系及三角洲物理模拟研究[D]. 四川:成都理工大学,2001. [Zhang Chunsheng. Physical simulation and relevant studies of the alluvial system and deltas[D]. Sichuan: Chengdu University of Technology, 2001.]
- [3] Clarke L E. Experimental alluvial fans: advances in understanding of fan dynamics and processes[J]. *Geomorphology*, 2015, 244: 135-145.
- [4] 张纪易. 粗碎屑洪积扇的某些沉积特征和微相划分[J]. *沉积学报*, 1985, 3(3): 75-85. [Zhang Jiyi. Some depositional characteristics and microfacies subdivision of coarse elastic alluvial fans[J]. *Acta Sedimentologica Sinica*, 1985, 3(3): 75-85.]
- [5] 郑占,吴胜和,许长福,等. 克拉玛依油田六区克下组冲积扇岩石相及储层质量差异[J]. *石油与天然气地质*, 2010, 31(4): 463-471. [Zheng Zhan, Wu Shenhe, Xu Changfu, et al. Lithofacies and reservoirs of alluvial fan in the lower Karamay Formation in the block-6 of Karamay oilfield, the Junggar Basin[J]. *Oil & Gas Geology*, 2010, 31(4): 463-471.]
- [6] 陈欢庆,舒治睿,林春燕,等. 粒度分析在砾岩储层沉积环境研究中的应用:以准噶尔盆地西北缘某区克下组冲积扇储层为例[J]. *西安石油大学学报(自然科学版)*, 2014, 29(6): 6-12, 34. [Chen Huanqing, Shu Zhirui, Lin Chunyan, et al. Application of grain-size analysis in research of sedimentary environment of conglomerate reservoir: Taking alluvial fan reservoir in the lower member of Kelamayi Formation in some area of the northwestern margin of Zhunger Basin as an example[J]. *Journal of Xi'an University (Natural Science Edition)*, 2014, 29(6): 6-12, 34.]
- [7] 吴胜和,范铮,许长福,等. 新疆克拉玛依油田三叠系克下组冲积扇内部构型[J]. *古地理学报*, 2012, 14(3): 331-340. [Wu Shenghe, Fan Zheng, Xu Changfu, et al. Internal architecture of alluvial fan in the Triassic Lower Karamay Formation in Karamay oilfield, Xinjiang[J]. *Journal of Palaeogeography*, 2012, 14(3): 331-340.]
- [8] 王晓光,贺陆明,吕建荣,等. 克拉玛依油田冲积扇构型及剩余油控制模式[J]. *断块油气田*, 2012, 19(4): 493-496. [Wang Xiaoguang, He Luming, Lü Jianrong, et al. Configuration of alluvial fan and control mode on remaining oil in Karamay oilfield[J]. *Fault-Block Oil & Gas Field*, 2012, 19(4): 493-496.]
- [9] 伊振林,吴胜和,杜庆龙,等. 冲积扇储层构型精细解剖方法:以克拉玛依油田六中区下克拉玛依组为例[J]. *吉林大学学报(地球科学版)*, 2010, 40(4): 939-946. [Yi Zhenlin, Wu Shenghe, Du Qinglong, et al. An accurate anatomizing method for structure of reservoir of alluvial fan: A case study on lower Karamay Formation, Lüzhong area, Karamay oilfield[J]. *Journal of Jilin University (Earth Science Edition)*, 2010, 40(4): 939-946.]
- [10] 包兴. 冲积扇构型建模方法研究[D]. 武汉:长江大学,2012. [Bao Xing. A research on alluvial fan architecture modeling method. Wuhan: Yangtze University, 2012.]
- [11] 陈欢庆,梁淑贤,舒治睿,等. 冲积扇砾岩储层构型特征及其对储层开发的控制作用:以准噶尔盆地西北缘某区克下组冲积扇储层为例[J]. *吉林大学学报(地球科学版)*, 2015, 45(1): 13-24. [Chen Huanqing, Liang Shuxian, Shu Zhirui, et al. Characteristics of conglomerate reservoir architecture of alluvial fan and its controlling effects to reservoir development: Taking alluvial fan reservoir in some area of northwest margin of Junggar Basin as an example[J]. *Journal of Jilin University (Earth Science Edition)*, 2015, 45(1): 13-24.]
- [12] 印森林,胡张明,郑丽君,等. 第四纪昌平冲积扇沉积特征研究[J]. *中国科技论文*, 2015, 10(15): 1828-1833. [Yin Senlin, Hu Zhangming, Zheng Lijun, et al. Sedimentary features of the Quaternary Changping alluvial fan[J]. *China Sciencepaper*, 2015, 10(15): 1828-1833.]
- [13] 冯文杰,吴胜和,徐长福,等. 冲积扇储层窜流通道及其控制的剩余油分布模式:以克拉玛依油田一中区下克拉玛依组为例[J]. *石油学报*, 2015, 36(7): 859-870. [Feng Wenjie, Wu Shenghe, Xu Changfu, et al. Water flooding channel of alluvial fan reservoir and its controlling distribution pattern of remaining oil: A case study of Triassic Lower Karamay Formation, Yizhong area, Karamay oilfield, NW China[J]. *Acta Petrolei Sinica*, 2015, 36(7): 859-870.]
- [14] 吴胜和,纪友亮,岳大力,等. 碎屑沉积地质体构型分级方案探讨[J]. *高校地质学报*, 2013, 19(1): 12-22. [Wu Shenghe, Ji Youliang, Yue Dali, et al. Discussion on hierarchical scheme of architectural units in clastic deposits[J]. *Geological Journal of China Universities*, 2013, 19(1): 12-22.]
- [15] 吴胜和,冯文杰,印森林,等. 冲积扇沉积构型研究进展[J]. *古地理学报*, 2016, 18(4): 497-512. [Wu Shenghe, Feng Wenjie, Yin Senlin, et al. Research advances in alluvial fan depositional architecture[J]. *Journal of Palaeogeography*, 2016, 18(4): 497-512.]
- [16] 冯文杰,吴胜和,夏钦禹,等. 基于地质质量信息的冲积扇储层沉积微相建模:以克拉玛依油田三叠系克下组为例[J]. *高校地质学报*, 2015, 21(3): 449-460. [Feng Wenjie, Wu Shenhe, Xia Qinyu, et al. Micro-facies modeling of alluvial fan reservoir based on geological vector information: A case study on the Triassic Lower Karamay Formation, Yizhong area, Karamay oilfield, NW China[J]. *Geological Journal of China Universities*, 2015, 21(3): 449-460.]
- [17] Yin S L, Wu S H, Feng W J, et al. Patterns of intercalation in alluvial fan reservoirs: A case study of Lower Karamay Formation, Yizhong Area, Karamay Oilfield, NW China[J]. *Petroleum Explo-*

- ration and Development, 2013, 40(6): 811-818.
- [18] Fidolini F, Ghinassi M, Aldinucci M, et al. Fault-sourced alluvial fans and their interaction with axial fluvial drainage: an example from the Plio-Pleistocene Upper Valdarno Basin (Tuscany, Italy) [J]. *Sedimentary Geology*, 2013, 289: 19-39.
- [19] DeCelles P G, Gray M B, Ridgway K D, et al. Controls on synorogenic alluvial-fan architecture, Beartooth Conglomerate (Palaeocene), Wyoming and Montana [J]. *Sedimentology*, 1991, 38(4): 567-590.
- [20] 朱筱敏. 沉积岩石学 [M]. 4 版. 北京: 石油工业出版社, 2008: 248-256. [Zhu Xiaomin. *Sedimentary petrology* [M]. 4th ed. Beijing: Petroleum Industry Press, 2008: 248-256.]
- [21] Waters J V, Jones S J, Armstrong H A. Climatic controls on late Pleistocene alluvial fans, Cyprus [J]. *Geomorphology*, 2010, 115 (3/4): 228-251.
- [22] Fernandez J, Bluck B J, Viseras C. The effects of fluctuating base level on the structure of alluvial fan and associated fan delta deposits: An example from the Tertiary of the Betic Cordillera, Spain [J]. *Sedimentology*, 1993, 40(5): 879-893.
- [23] Calvo R, Ramos E. Unlocking the correlation in fluvial outcrops by using a DOM-derived virtual datum: Method description and field tests in the Huesca fluvial fan, Ebro Basin (Spain) [J]. *Geosphere*, 2015, 11(5): 1507-1529.
- [24] Carnicelli S, Benvenuti M, Andreucci S, et al. Late Pleistocene relic Ultisols and Alfisols in an alluvial fan complex in coastal Tuscany [J]. *Quaternary International*, 2015, 376: 163-172.
- [25] Blair T C. Sedimentology of the debris-flow-dominated Warm Spring Canyon alluvial fan, Death Valley, California [J]. *Sedimentology*, 1999, 46(5): 941-965.
- [26] Kim B C, Lowe D R. Depositional processes of the gravelly debris flow deposits, South Dolomite alluvial fan, Owens Valley, California [J]. *Geosciences Journal*, 2004, 8(2): 153-170.
- [27] Haas T, Braat L, Leuven J R F W, et al. Effects of debris flow composition on runout, depositional mechanisms, and deposit morphology in laboratory experiments [J]. *Journal of Geophysical Research: Earth Surface*, 2015, 120(9): 1949-1972.
- [28] Harvey A M. The role of base-level change in the dissection of alluvial fans: case studies from southeast Spain and Nevada [J]. *Geomorphology*, 2002, 45(1/2): 67-87.
- [29] Cuevas Martínez J L, Pérez L C, Marcuello A, et al. Exhumed channel sandstone networks within fluvial fan deposits from the Oligo-Miocene Caspe Formation, South-east Ebro Basin (North-east Spain) [J]. *Sedimentology*, 2010, 57(1): 162-189.
- [30] Stanistreet I G, McCarthy T S. The Okavango Fan and the classification of subaerial fan systems [J]. *Sedimentary Geology*, 1993, 85(1/2/3/4): 115-133.
- [31] Ridgway K D, Decelles P G. Stream-dominated alluvial fan and lacustrine depositional systems in Cenozoic strike-slip basins, Denali fault system, Yukon Territory, Canada [J]. *Sedimentology*, 1993, 40(4): 645-666.
- [32] Allen P A. Sediments and processes on a small stream-flow dominated, devonian alluvial fan, shetland islands [J]. *Sedimentary Geology*, 1981, 29(1): 31-37, 48-66.
- [33] de Haas T, Ventra D, Carbonneau P E, et al. Debris-flow dominance of alluvial fans masked by runoff reworking and weathering [J]. *Geomorphology*, 2014, 217: 165-181.
- [34] de Haas T, Kleinhans M G, Carbonneau P E, et al. Surface morphology of fans in the high-Arctic periglacial environment of Svalbard: controls and processes [J]. *Earth-Science Reviews*, 2015, 146: 163-182.
- [35] Blair T C. Sedimentary processes and facies of the waterlaid Anvil Spring Canyon alluvial fan, Death Valley, California [J]. *Sedimentology*, 1999, 46(5): 913-940.
- [36] 胡杨, 夏斌, 郭峰, 等. 新疆和什托洛盖盆地构造演化特征及其对油气成藏的影响 [J]. *地质与资源*, 2012, 21(4): 380-385. [Hu Yang, Xia Bin, Guo Feng, et al. Tectonic evolution and its influence on hydrocarbon accumulation of Heshituoluogai Basin in northwest Xinjiang [J]. *Geology and Resources*, 2012, 21(4): 380-385.]
- [37] 胡杨, 郭峰, 刘见宝, 等. 和什托洛盖盆地构造演化及油气成藏条件 [J]. *西南石油大学学报 (自然科学版)*, 2011, 33(5): 68-74. [Hu Yang, Guo Feng, Liu Jianbao, et al. Analysis of tectonic evolution and oil-gas reservoir formation condition of Heshituoluogai Basin in northwest Xinjiang [J]. *Journal of Southwest Petroleum University (Science & Technology Edition)*, 2011, 33(5): 68-74.]
- [38] 吕辉河. 新疆西准噶尔白杨河流域地貌特征及演化分析 [D]. 济南: 鲁东大学, 2013. [Lü Huihe. *Analysis of geomorphic features and evolution of Baiyanghe River in West Junggar, Xinjiang, China* [D]. Ji'nan: Ludong University, 2013.]
- [39] Miall A D. Architectural-element analysis: a new method of facies analysis applied to fluvial deposits [J]. *Earth-Science Reviews*, 1985, 22(4): 261-308.
- [40] Postma G, Nemeč W, Kleinspehn K L. Large floating clasts in turbidites: a mechanism for their emplacement [J]. *Sedimentary Geology*, 1988, 58(1): 47-61.
- [41] Nemeč W, Steel R J. Alluvial and coastal conglomerates: their significant features and some comments on gravelly mass-flow deposits [M]//Koster E H, Steel R J. *Sedimentology of Gravels and Conglomerates*. Canadian: Canadian Society of Petroleum Geologists, 1984: 1-31.
- [42] Franke D J, Hornung J, Hinderer M. A combined study of radar facies, lithofacies and three-dimensional architecture of an alpine alluvial fan (Illgraben fan, Switzerland) [J]. *Sedimentology*, 2015, 62(1): 57-86.
- [43] Boothroyd J C, Ashley G M. Processes, bar morphology, and sedimentary structures on braided outwash fans, Northeastern Gulf of Alaska [M]//Jopling A V, McDonald B C. *Glaciofluvial and Glaciolacustrine Sedimentation*. Tulsa, Okla: Society of Economic Paleontologists and Mineralogists, 1975: 193-222.
- [44] Hein F J, Walker R G. Bar evolution and development of stratification in the gravelly, braided, Kicking Horse River, British Colum-

- bia[J]. Canadian Journal of Earth Sciences, 1977, 14(4): 562-570.
- [45] Todd S P. Stream-driven, high-density gravelly traction carpets: possible deposits in the Trabeg Conglomerate Formation, SW Ireland and some theoretical considerations of their origin[J]. Sedimentology, 1989, 36(4): 513-530.
- [46] Tunbridge I P. Facies model for a sandy ephemeral stream and clay playa complex; the Middle Devonian Trentishoe Formation of North Devon, U.K.[J]. Sedimentology, 1984, 31(5): 697-715.
- [47] Alçiçek H, Jiménez-Moreno G. Late Miocene to Plio-Pleistocene fluvio-lacustrine system in the Karacasu Basin (SW Anatolia, Turkey): depositional, paleogeographic and paleoclimatic implications [J]. Sedimentary Geology, 2013, 291: 62-83.
- [48] McCarthy T S, Cadle A B, Blair T C, et al. Alluvial fans and their natural distinction from rivers based on morphology, hydraulic processes, sedimentary processes, and facies assemblages; discussion and reply [J]. Journal of Sedimentary Research, 1995, 65(3): 581-586.
- [49] Blair T C. Sedimentology and progressive tectonic unconformities of the sheetflood-dominated Hell's Gate alluvial fan, Death Valley, California[J]. Sedimentary Geology, 2000, 132(3/4): 233-262.
- [50] Miall A D. The geology of fluvial deposits[M]. Berlin: Springer, 1996: 582-583.
- [51] Shukla U K. Sedimentation model of gravel-dominated alluvial piedmont fan, Ganga Plain, India [J]. International Journal of Earth Sciences, 2009, 98(2): 443-459.
- [52] Shukla U K, Singh I B, Sharma M, et al. A model of alluvial megafan sedimentation: Ganga Megafan[J]. Sedimentary Geology, 2001, 144(3/4): 243-262.

Research on Lithofacies Types, Cause Mechanisms and Distribution of a Gravel Braided-River Alluvial Fan: A case study of the modern Poplar River alluvial fan, northwestern Junggar Basin

JIN Jun^{1,2}, LIU DaWei^{1,3}, JI YouLiang¹, YANG Zhao², GAO ChongLong¹, WANG Jian², DUAN XiaoBing¹, HUAN ZhiJun¹, LUO NiNa¹

1. College of Geosciences, China University of Petroleum (Beijing), Beijing 102249, China

2. PetroChina Xinjiang Oilfield Company, Research Institute of Experiment and Detection, Karamay, Xinjiang 834000, China

3. Institute of Geology and Geophysics, Chinese Academy of Sciences, Beijing 100029, China

Abstract: Conglomerate reservoirs in alluvial fans are an important oil and gas reservoir type in the Junggar Basin. However, alluvial fan glutinite reservoirs consist of several lithofacies and poor continuity, which causes the lithofacies interpretation of the alluvial fan facies to be a fundamental and difficult research area. As an example, the lithofacies mechanism and distribution of the modern Poplar River alluvial fan at the northwestern margin of the Junggar Basin is discussed on the basis of a large amount of outcrop data, source rocks, hydrological data and alluvial fan studies reported in the literature. According to the deposition mechanism, the Poplar River alluvial fan is a braided-river alluvial fan with features typical of its large scale (fan total area is 327.6 km²), gentle slope (about 4‰-7‰), and rough sediments. Sixteen lithofacies were recognized; their hydrodynamic differences indicate that they may be classified into five causes: debris flow, high-flow traction current, low-flow traction current, hydrostatic deposition, and aeolian deposition. Debris flow is mainly composed of flood deposits; high-flow traction current mainly includes sheet-flood deposits and turbulent deposits; low-flow traction current is mainly composed of (gravelly) sand channel sediments; hydrostatic deposits are dominated by fine material, and aeolian deposits mainly consist of wind-transported sediments. The lithofacies are divided into four types according to sedimentary structure, granularity and distribution scale. The first type has an obvious sedimentary structure and wide distribution. The second type has obvious sedimentary structural characteristics but limited distribution. The third type, which is present on a large scale, has characteristics in which the sedimentary structures are not apparent. The sedimentary structure and physical properties of the fourth type are also not apparent, and occur only on a limited scale. The first and second types of lithofacies are mainly caused by traction currents that mainly form in the middle and distal parts of the flood period, and in the middle part of the inter-flood stage; those lithofacies form higher-quality reservoirs underground in due course.

Key words: braided-river alluvial fan; lithofacies types; granularity characteristic; lithofacies distribution; open-framework conglomerate